

**BacM, an N-terminally processed bactofilin of *Myxococcus xanthus*,
is crucial for proper cell shape**

Matthias K. Koch, Colleen A. McHugh, and Egbert Hoiczyk*

The W. Harry Feinstone Department of Molecular Microbiology and Immunology,
Johns Hopkins Bloomberg School of Public Health, Baltimore, MD 21205, USA

*Corresponding Author, 615 N Wolfe St, E2624, Baltimore, MD 21205, USA

Phone: 443-287-2898; Fax: 410-955-0105; Email: ehoiczyk@jhsp.h.edu

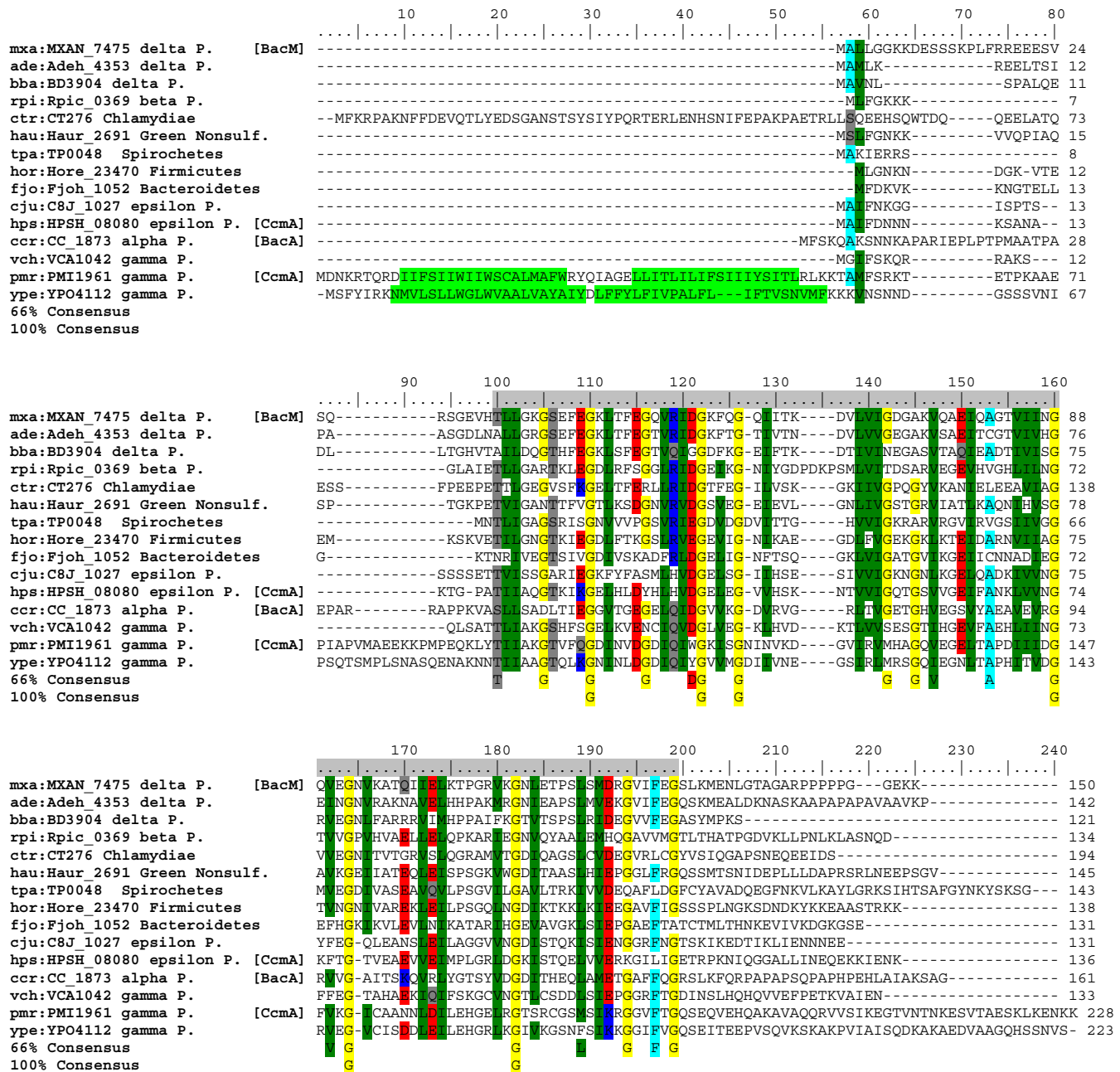


Fig. S1A. Alignment of BacM (MXAN_7475) with homologues from various phyla. The aligned protein sequences were chosen to represent species from a comprehensive variety of phyla. They were selected from a phylogenetic tree of putative BacM orthologues created by the KEGG server with the "best-best search method" (<http://www.genome.jp/kegg/>; Fig. S2, marked by asterisks). All contain the DUF583 domain, indicated by light grey highlighting. Note the good conservation of glycine residues of which six are conserved in 100% of the aligned species. N-terminal hydrophobic regions qualifying for transmembrane helices are highlighted in light green. Alignment and amino acid color code were generated by BioEdit 7.0 sequence alignment software (<http://www.mbio.ncsu.edu/bioedit/>). Species are: mx: *Myxococcus xanthus*, ade: *Anaeromyxobacter dehalogenans*, bba: *Bdellovibrio bacteriovorus*, rpi: *Ralstonia pickettii*, ctr: *Chlamydia trachomatis*, hau: *Herpetosiphon aurantiacus*, tpa: *Treponema pallidum*, hor: *Halothermothrix orenii*, fjo: *Flavobacterium johnsoniae*, cju: *Campylobacter jejuni*, hps: *Helicobacter pylori*, ccr: *Caulobacter crescentus*, vch: *Vibrio cholerae*, pmr: *Proteus mirabilis*, ype: *Yersinia pestis*. Taxonomic groups are listed behind the protein names (P., proteobacteria; Nonsulf., nonsulfur bacteria). Alternative names for proteins, as reported in this study, are indicated in brackets.

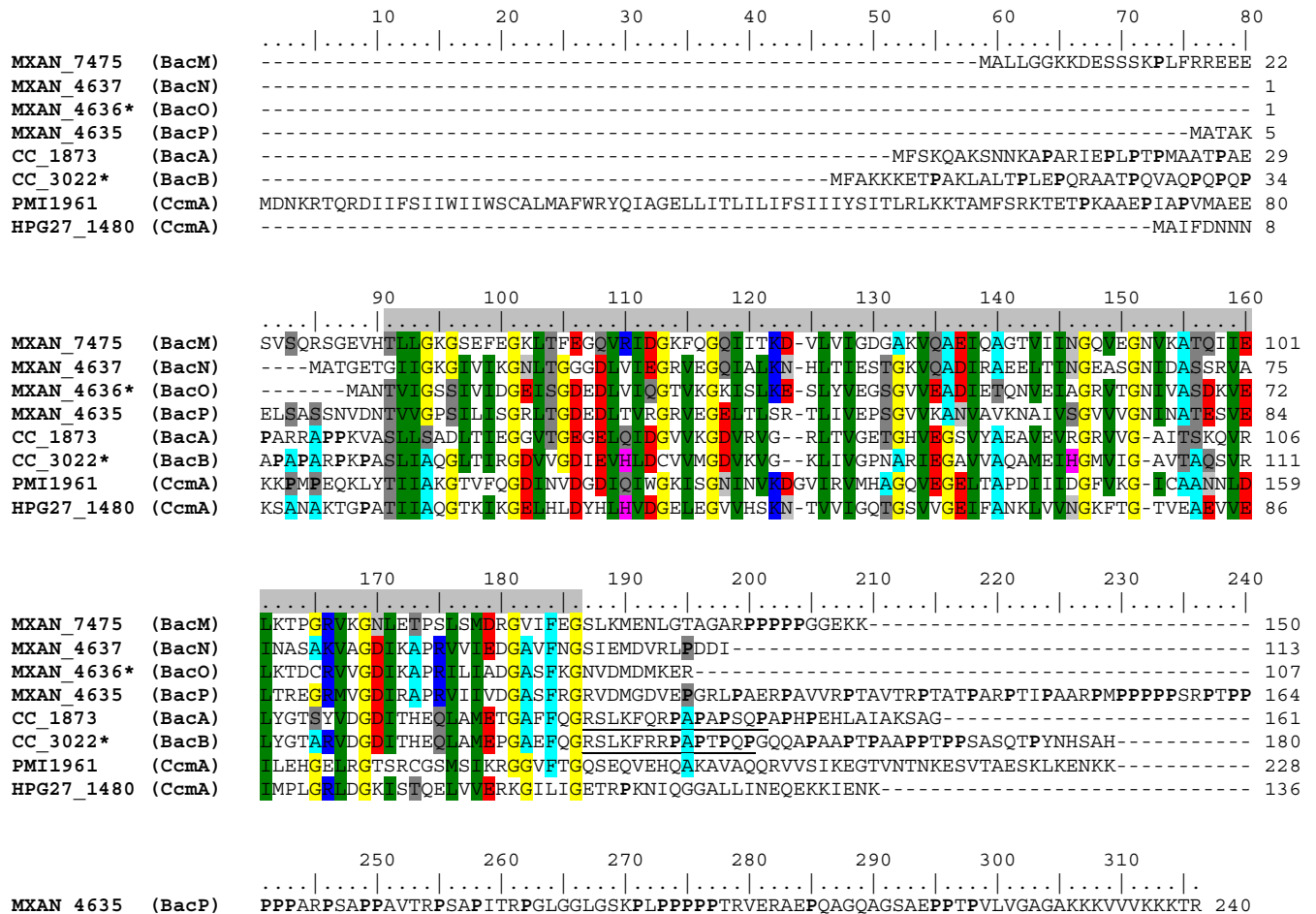


Fig. S1B. Alignment of BacM-P (*M. xanthus*) with BacA and BacB (*C. crescentus*), CcmA (*P. mirabilis*) and CcmA (*H. pylori*). The conserved DUF583 domain is highlighted in light grey. Proline residues outside of the DUF583 domain are highlighted bold. Asterisks indicate shortening of the assigned open reading frames. CC_3022 was shortened to BacB (Kühn *et al.*, 2010); MXAN_4636 was shortened from 126 to 107 amino acids to result in BacO based on homology to its orthologue STIAU_7480 from *S. aurantiaca*. Alignment and amino acid color code were generated by BioEdit 7.0 software by using the PAM120 matrix and 60% shading cutoff. Note the absence of significant similarity for the N- and C-terminal regions outside the DUF583 domains of these bacteriophages (except for the first part of the BacA/B C-terminal regions as highlighted by underlining).

Table S1. Length and proline content of the N- and C-terminal regions outside of the DUF583 domains of the bacteriophages shown in Fig. S1B.

Bacteriophage	Number of N-terminal residues (number of prolines)	Number of C-terminal residues (number of prolines)
BacM (<i>M. xanthus</i>)	32 (1)	23 (5)
BacN (<i>M. xanthus</i>)	6 (0)	12 (1)
BacO (<i>M. xanthus</i>)	3 (0)	9 (0)
BacP (<i>M. xanthus</i>)	15 (0)	130 (36)
BacA (<i>C. crescentus</i>)	39 (8)	29 (6)
BacB (<i>C. crescentus</i>)	44 (11)	43 (12)
CcmA (<i>P. mirabilis</i>)	90 (5)	43 (0)
CcmA (<i>H. pylori</i>)	18 (1)	24 (1)

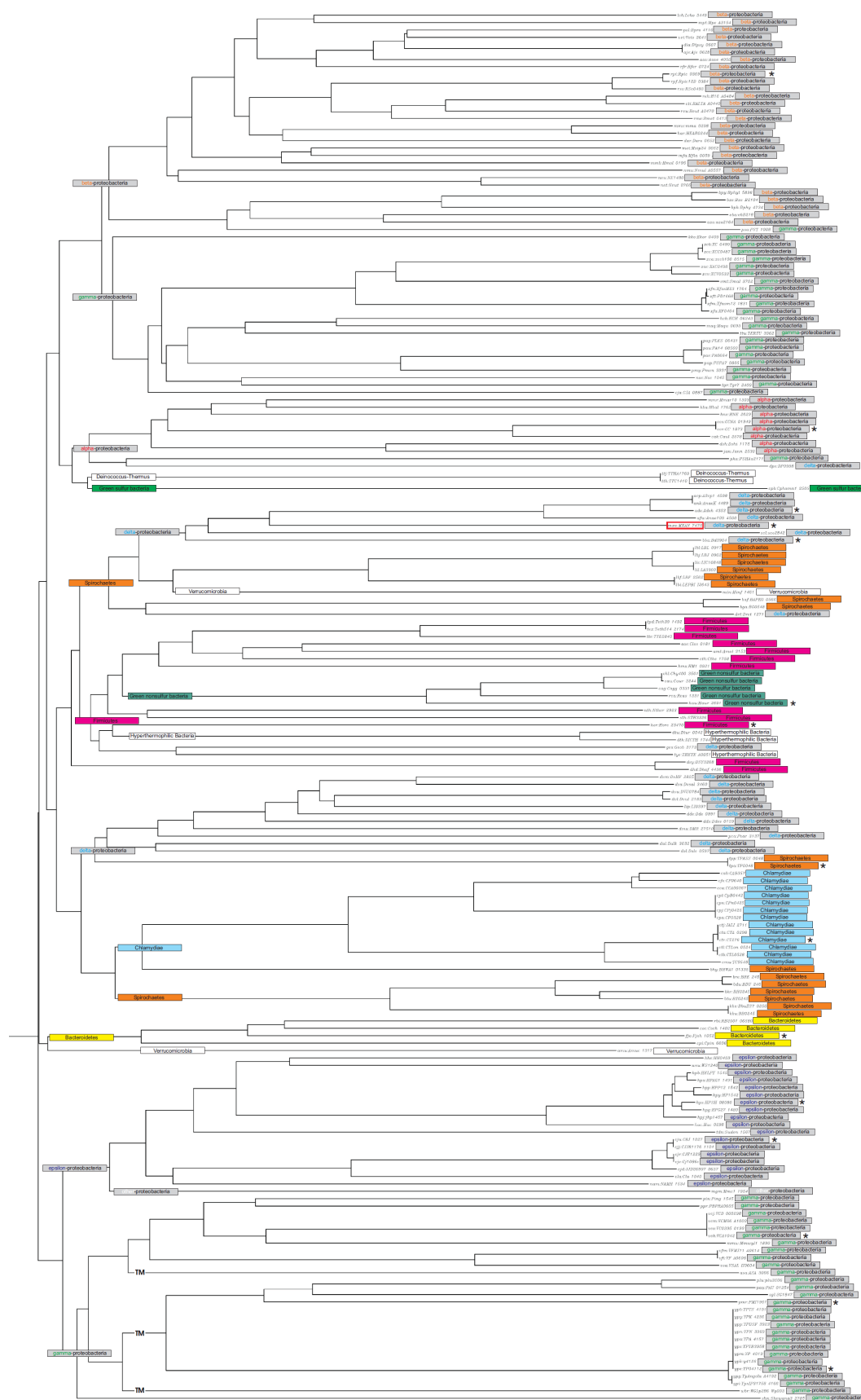


Fig. S2. Phylogenetic tree of putative MXAN_7475 (BacM) orthologues produced by the KEGG server via the "best-best search method" (<http://www.genome.jp/kegg/>). Taxonomic descriptions added manually (boxes). Branches of species in which the encoded bactofilin contains putative transmembrane regions are marked (TM).

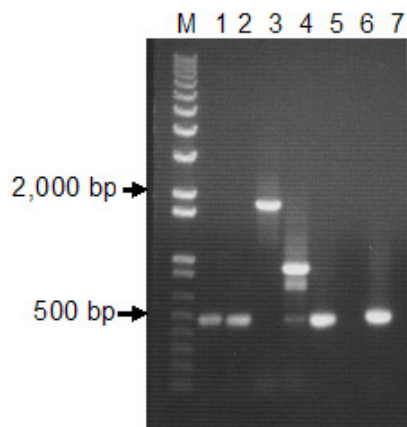


Fig. S3. Analysis of the putative operon *MXAN_7477-7474*. PCR reactions to verify a contiguous cDNA fragment between the primer locations were performed as described below. PCR products are shown on a 0.8% agarose gel. M, marker; lane 1, *parA-parB*; lane 2, *parB-bacM*; lane 3, *parA-MXAN_7474*; lane 4, *parB-MXAN_7474*; lane 5, *bacM-MXAN_7474*; lane 6, negative control; lane 7, positive control 500 bp fragment of the *M. xanthus gyrB* housekeeping gene.

Total cellular RNA was extracted from log phase cultures of *M. xanthus* strain DK1622 using the MasterPure RNA extraction kit (Epicentre Biotechnologies) and reverse transcribed to cDNA. PCR reactions to analyze the putative operon *MXAN_7477-7474* were performed with primers CM336 and CM337 (*parA* to *parB*, 481 bp), CM338 and CM339 (*parB* to *bacM*, 476 bp), CM340 and CM341 (*bacM* to *MXAN_7474*, 475 bp) using cDNA as a template, to confirm that transcripts containing sequence from each of the genes was contained on the same cDNA fragment. As positive control a primer set (CM327 and CM328) was designed to amplify a 500 bp fragment of *gyrB* gene. The negative control was the same reaction, but without the addition of polymerase.

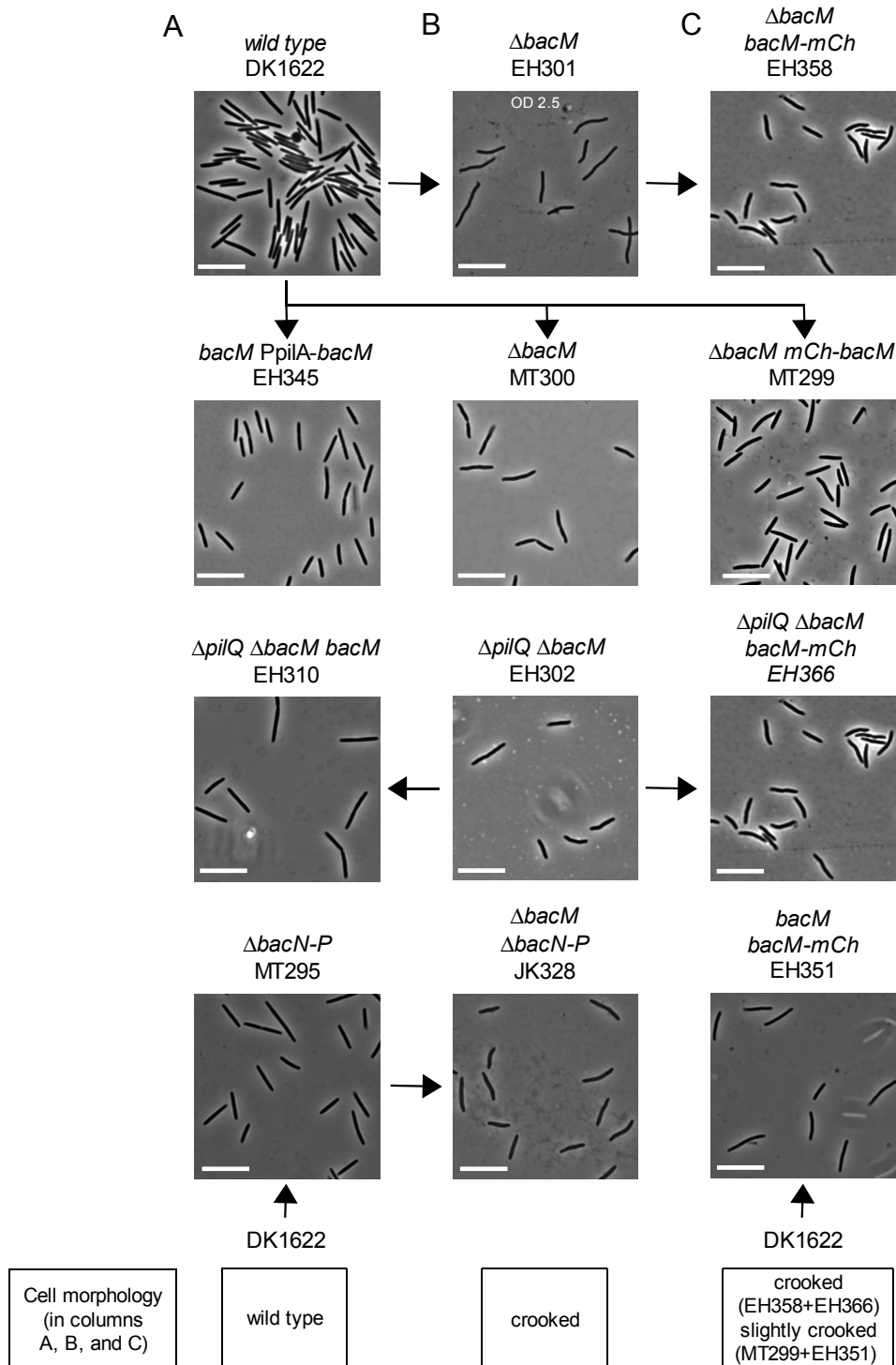


Fig. S4. Cell morphology of bactofilin mutants. Phase contrast light micrographs of cells from liquid CTT cultures at mid-logarithmic growth phase or at the indicated OD_{600} . Relevant genotypes and strain names are indicated. Bars represent 10 μm . (A) Strains containing the wild-type *bacM* gene. (B) Strains deleted in *bacM*. (C) Strains expressing gene fusions of *bacM* and *mCherry*. Arrows indicate the parent strain / daughter strain relationships. Note that all strains lacking the *bacM* gene have a pronounced crooked morphology with the exception of strain MT299 which shows only slight crookedness. However, immunoblot analysis of MT299 showed that it contained full length and truncated BacM in addition to the encoded mCherry-BacM fusion protein (Fig. S5D).

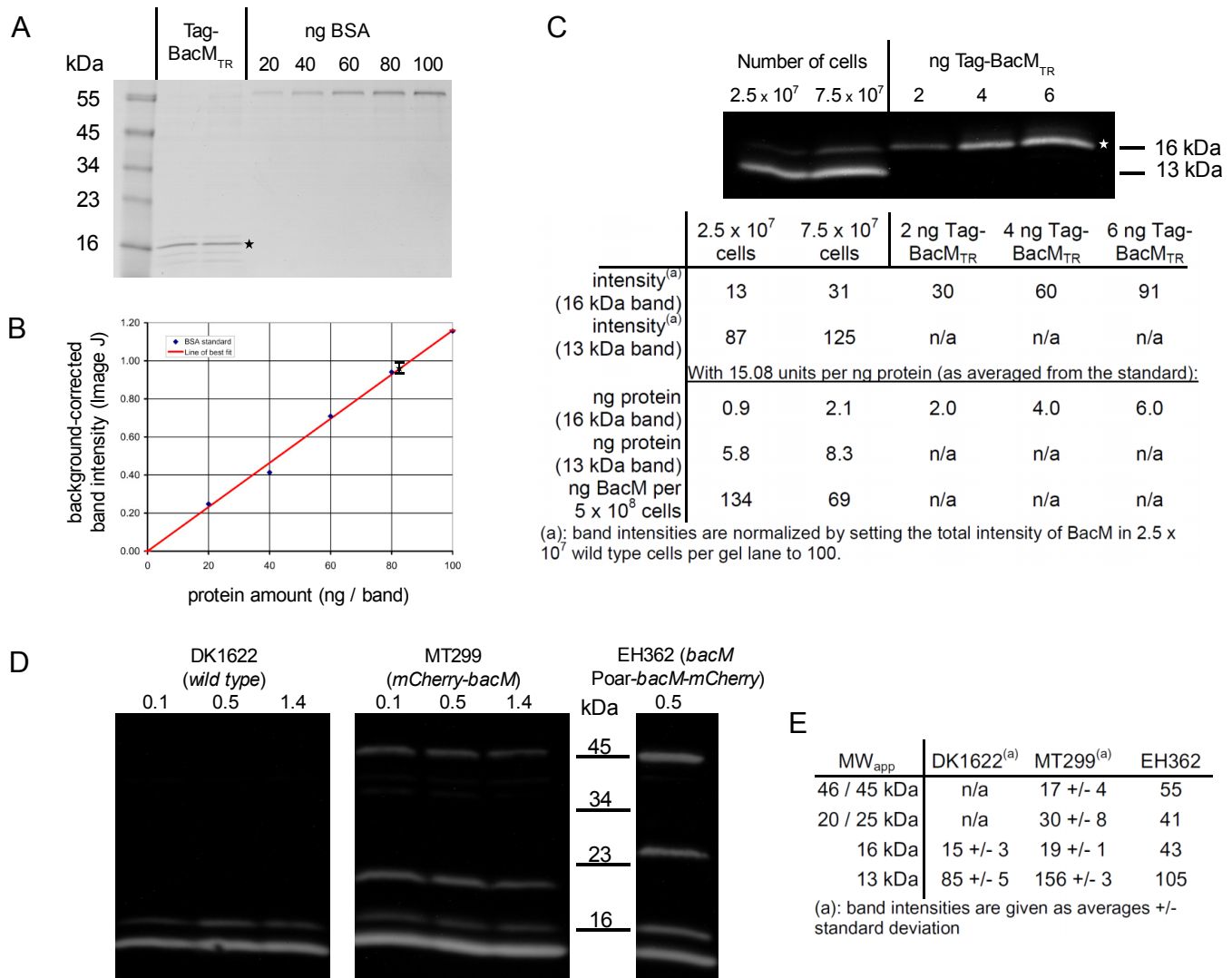


Fig. S5. Quantification of BacM. (A) Scan of a Coomassie Blue R250-stained SDS PAGE gel containing defined amounts of bovine serum albumin (BSA) and of purified hexahistidine-V5-TEV-tagged truncated BacM lacking amino acids 1 to 27 (Tag-BacM_{TR}). After inversion of the image, Image J software (<http://rsbweb.nih.gov/ij>) was used to quantify the intensities of the gel bands. (B) Standard curve of the BSA band intensities after background correction. Thirteen microliters of a diluted sample of purified Tag-BacM_{TR} contained 82 (+/- 2) ng of the major protein species (asterisk) running at 16 kDa (background-corrected relative intensity of 0.97 +/- 0.03). This corresponds to a concentration of 6.3 (+/- 0.2) ng/ml of the 16 kDa species in the sample. (C) Chemiluminescence image of an immunoblot of total protein from 2.5 x 10⁷ and 7.5 x 10⁷ DK1622 cells, and of 2, 4, and 6 ng of Tag-BacM_{TR} (of the sample from A) as a quantification standard. The table lists the relative band intensities as determined with ImageJ, and the calculated ng of BacM per band and per 5 x 10⁸ cells (corresponding to 1 ODml cells). (D) Chemiluminescence image of immunoblots of total protein from 6 x 10⁷ cells of the indicated strains at different growth phases (OD₆₀₀ ranging from 0.1 to 1.4). Note the presence of 16 and 13 kDa bands not only for DK1622 and EH362, which both encode wild-type BacM, but also for MT299, in which *bacM* is replaced by *mCherry-bacM* (Kühn *et al.*, 2010). Strains MT299 and EH362 produce bands at apparent MWs of 46 and 45 kDa, respectively, consistent with encoded fusions of BacM and mCherry. They additionally produce bands at apparent MWs of 20 and 25 kDa, respectively. These species are recognized by anti-BacM, and are smaller than mCherry (27 kDa) and larger than BacM. This suggests that they contain the entirety or a part of BacM, plus a part of mCherry. (E) Relative intensities of the bands shown in D. As in C, the values for the band intensities are normalized to set the combined intensities of 16 and 13 kDa bands in DK1622 to 100.

Fig. S5 (continued):

Calculation of the number of BacM molecules per cell when 5×10^8 cells (corresponding to 1 ml cell suspension of $OD_{600} = 1$) contain 134 ng BacM

As a saturation effect was frequently observed when quantifying protein in increasingly intense immunoblot bands, we assume that the actual amount of BacM is closer to the higher value of 134 ng per 5×10^8 cells, which was determined from the less intense bands on the immunoblot (Fig. S5C). If 5×10^8 cells contain 134 ng BacM, then one single cell contains: 2.68×10^{-16} g. One molecule of the more abundant BacM_{TR} has a mass of 13 kDa corresponding to 2.16×10^{-20} g (1 Da = 1.66×10^{-24} g).

Therefore one cell should contain: $2.68 \times 10^{-16} / 2.16 \times 10^{-20} = 12,400$ molecules BacM. When calculating with the lower determined value of 69 ng per 5×10^8 cells (Fig. S5C), the calculated number of BacM per cell is 6,400.

Calculation of the number of BacM molecules per cell when assuming an average cell of 4 μ m length with a 6 μ m bundle of 5 - 8 individual fibers, and 3 nm as the length of a subunit

Considering that the BacM cables span the entire cell, the length of a hypothetical single fiber winding through a 4 μ m cell is assumed to be approximately 6 μ m. The conserved DUF583 domain of bactofilins and the C-terminal domain of MinC both contain roughly 100 amino acids. As both domains contain frequent glycine residues arranged with similar spacing, the DUF583 domain might structurally resemble the beta helix formed by this MinC domain (Cordell *et al.*, 2001). Based on the dimensions of the MinC domain crystal structure, a BacM molecule is likely to be just slightly larger than 3 x 3 x 3 nm. Using these data, about 2,000 BacM molecules would form a hypothetical cell-spanning single fiber. When assuming that the cytoplasmic cables are formed by bundles of 5 - 8 individual fibers similar to those present in fiber isolations (Fig. 1), then the number of BacM copies per cell can be estimated to be in the range of 10,000 to 16,000.

The experimentally determined number of 6,400, and especially the more likely number of 12,400 molecules BacM per cell would therefore be consistent with the existence of a cable of several individual fibers winding across the total length of the cell.

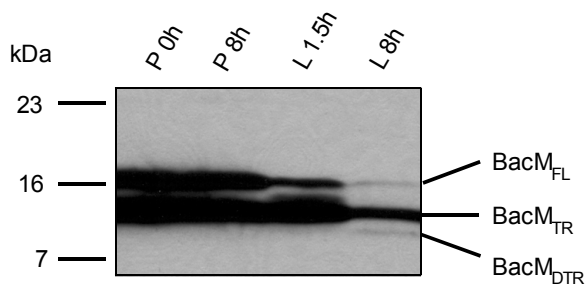


Fig. S6. Proteolysis of BacM in cell lysates in the absence of protease inhibitors. Anti-BacM immunoblot showing different forms of BacM. Cell pellet (P), or lysate after sonication in water without protease inhibitors (L). Samples were frozen in liquid nitrogen immediately (0 h), or after 1.5 h or 8 h at 25°C, as indicated. Proteins were dissolved by boiling in Laemmli buffer for 20 min. The positions of the full length (BacM_{FL}), N-terminally truncated (BacM_{TR}), and N- and C-terminally truncated (BacM_{DTR}) versions of BacM are indicated.

The immunoblots showed only two bands at the MWs of BacM_{FL} and BacM_{TR} when the cells were immediately frozen in liquid nitrogen, either directly after pelleting or after keeping the intact cell pellet for 8 hours at 25°C.

However, when the cells were sonicated and left at room temperature for various periods of time the amount of the full-length form and that of the truncated form decreased over time and a band appeared at the MW of the double-truncated (BacM_{DTR}) form.

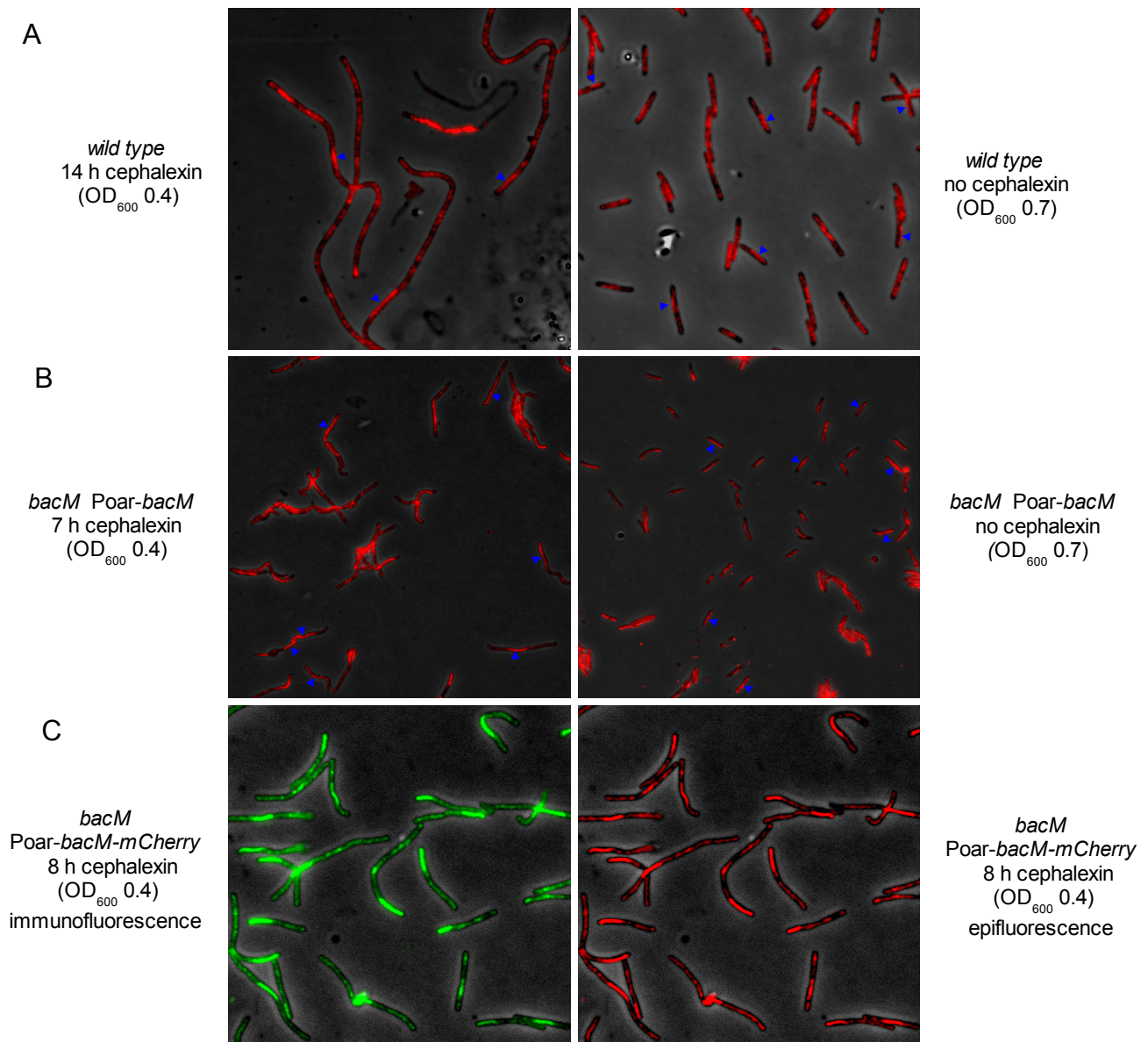


Fig. S7. In addition to helix-like cables, BacM forms lateral rod-like structures in cells expressing or moderately overexpressing *bacM*, and screw-shaped structures in cells moderately overexpressing *bacM*-*mCherry*. Overlays of phase contrast and immunofluorescence micrographs of cells grown for different times in CTT medium with 100 μ M cephalaxin or in CTT medium alone to the indicated ODs. Primary antibody was anti-BacM, secondary antibodies were either (red) AlexaFluor594- or (green) AlexaFluor488-coupled anti-rabbit-IgG. (A) Cephalaxin-treated elongated wild-type cells (DK1622) frequently contained a rod-like structure either near the cell pole or towards the center of the cell (the cell containing a bright and a dark half had undergone lysis). After growth in CTT medium, a certain fraction of the cells (generally between 20 and 30 %) contained a rod-like structure, usually located at one side of the cell near a pole. Its length was variable mostly between 1.5 and 4 μ m. Blue arrows mark the rods. (B) Cells moderately overexpressing *bacM* from the *oar* promoter (strain EH344) also contained such rods starting from a pole, or when treated with cephalaxin also in the center of the cell. Compared to wild-type cells, these rods were significantly longer and more frequent. The difference was especially notable for cells grown in CTT alone. (C) Cells of strain EH362, moderately overexpressing *bacM*-*mCherry* from the *oar* promoter in a wild-type background, after growth in cephalaxin and fixation. In addition to apparent cables, these cells contain a single screw-shaped structure per cell, mostly at the cell pole but also frequently near the cell center. Immunofluorescence with anti-BacM and epifluorescence of *mCherry* show colocalization. This demonstrates that both, the cables and the screws, are formed by the fusion protein, and that the immunofluorescence experiments accurately reflect the localization of BacM in the cells.

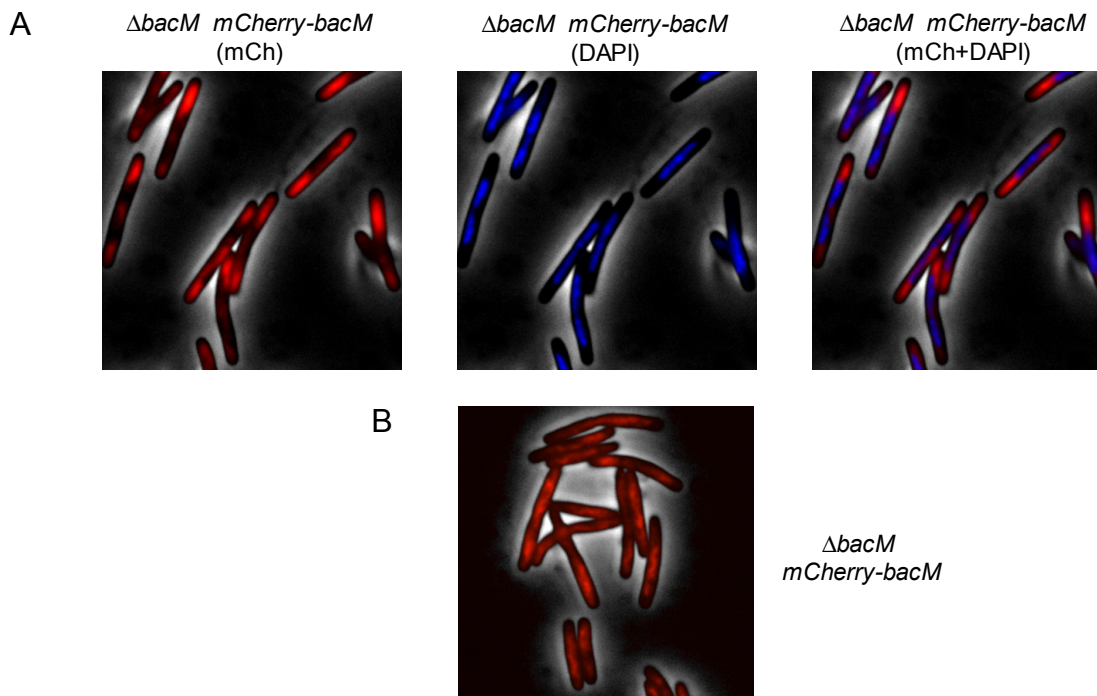


Fig. S8. (A) Cells of mCherry-BacM producing strain MT299 (Kühn *et al.*, 2010), harvested at mid-logarithmic growth phase and stained with DNA stain DAPI. Shown are overlays of the phase contrast image with the red mCherry fluorescence signal (mCh), the blue DAPI signal (DAPI) and both (mCh+DAPI). Note that the cellular locations lacking significant mCherry fluorescence colocalize with the DAPI signal. (B) Cells of strain MT299 after fixation. **Supplementary Video 3** shows a succession of optical sections through the fixed cells.

Supplementary Videos:

When it became obvious during the acquisition of epifluorescence pictures that the clusters seen in Fig. 5A were moving inside the cells, we decided to study their movement *in vivo* (**Supplementary Videos 1 and 2**). Pictures were recorded at 500 ms or 3 s intervals using cells after extended growth on agar plates or at stationary growth phase, as these cells were found to be least susceptible to photo bleaching. While some fluorescent clusters maintained a fixed position in the cell, others showed vigorous back and forth movement. An alternative explanation for the moving entities between stationary clusters might be that they consist of BacM-mCherry cables, which are "swinging" back and forth inside the cell. This interpretation would explain why cables become easily visible only after fixation (e.g. Fig. S8B). They would produce only diffuse fluorescence in unfixed cells (e.g. Fig. S8A), as the movement of unfixed cables across the cell during image acquisition would diffuse their signal, making the cable structure practically invisible to the camera. As the cellular visualization of BacM in the absence of mCherry requires fixation, it remains open whether the native BacM cables are moving within the cytoplasm.

Video 1: EH358 ($\Delta bacM$ *bacM-mCherry*) cells from CTT agar plate 20 days after plating. Red fluorescence recorded at 2 exposures per second for 50 s. Video shows 8 frames per second (fps). Result: 50 s shown in ~12 s, i.e. 4 x faster than real time.

Video 2: EH358 ($\Delta bacM$ *bacM-mCherry*) cells from CTT culture at OD_{600} of 1.60. Red fluorescence recorded at 20 exposures per minute for 1 min. Video shows 5 fps. Result: 60 s shown in 4 s, i.e. 15 x faster than real time.

Video 3: Sequence of 11 optical sections through the cells shown in Fig. S8B, recorded in the red channel and followed by the same sequence after deconvolution for easier visualization (100 nm slicing distance). The continuous directional displacement of fluorescence signals as seen in the video is consistent with what would be expected for mCherry-BacM / BacM1 cables winding through the cell. Examples of such displacements are seen for example to the right of the three white lines (line thickness is that of 1 pixel of the original picture, 65 nm).

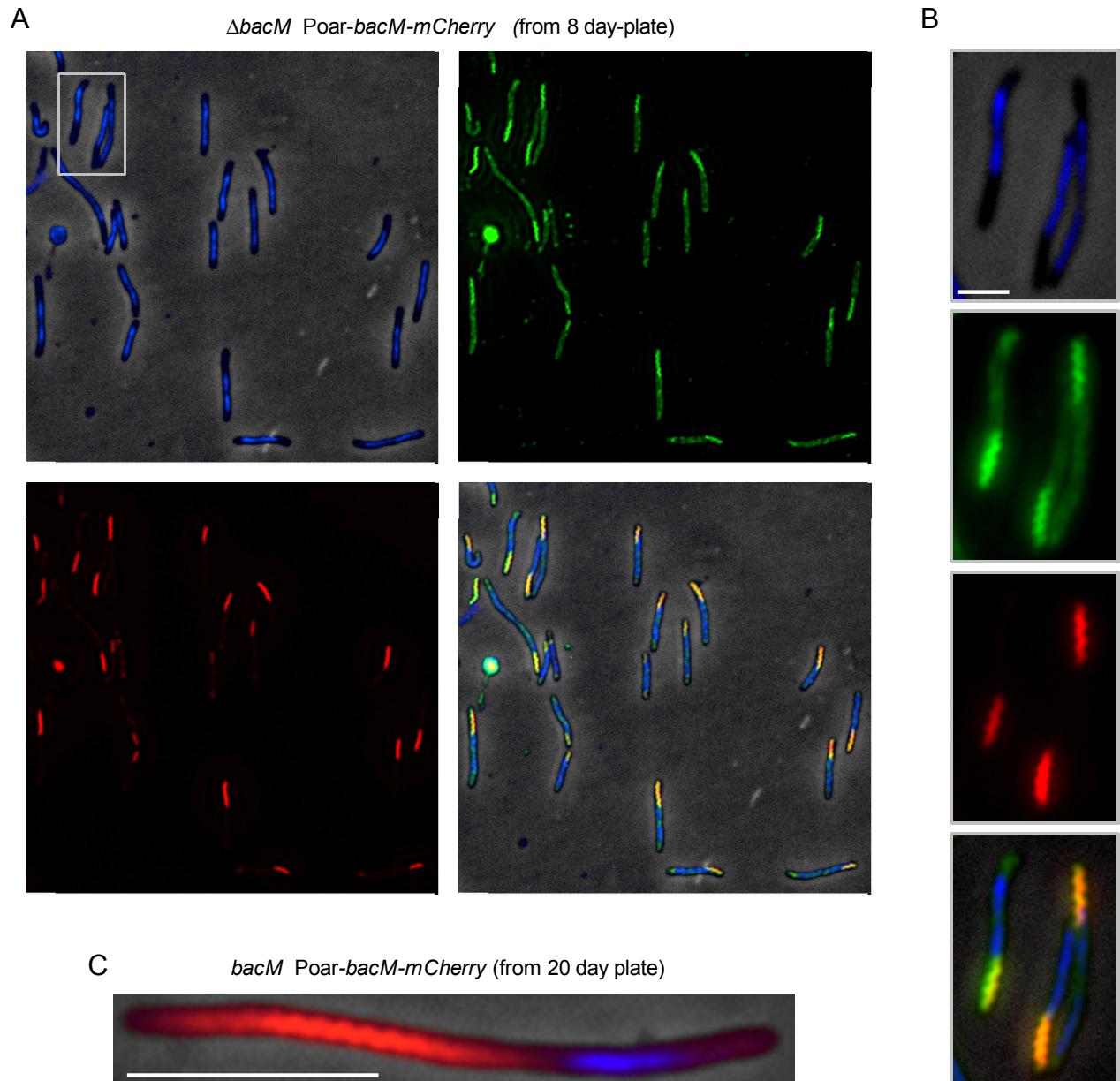


Fig. S9. Visualization of BacM-mCherry screws and DNA in cells collected from CTT agar plates. (A) Cells of strain EH364 after fixation. DAPI staining (blue) on phase contrast, anti-BacM immunofluorescence (green), mCherry fluorescence (red), and overlay on phase contrast. Images are shown after deconvolution. (B) Magnification of the region marked by the grey box in A. Images are shown without deconvolution. (C) Unfixed cell of strain EH362. The bars in B and C represent 2 and 6 μm , respectively. Note that DNA staining and screw localization are not overlapping, suggesting that screw growth might result in the displacement of cellular DNA.

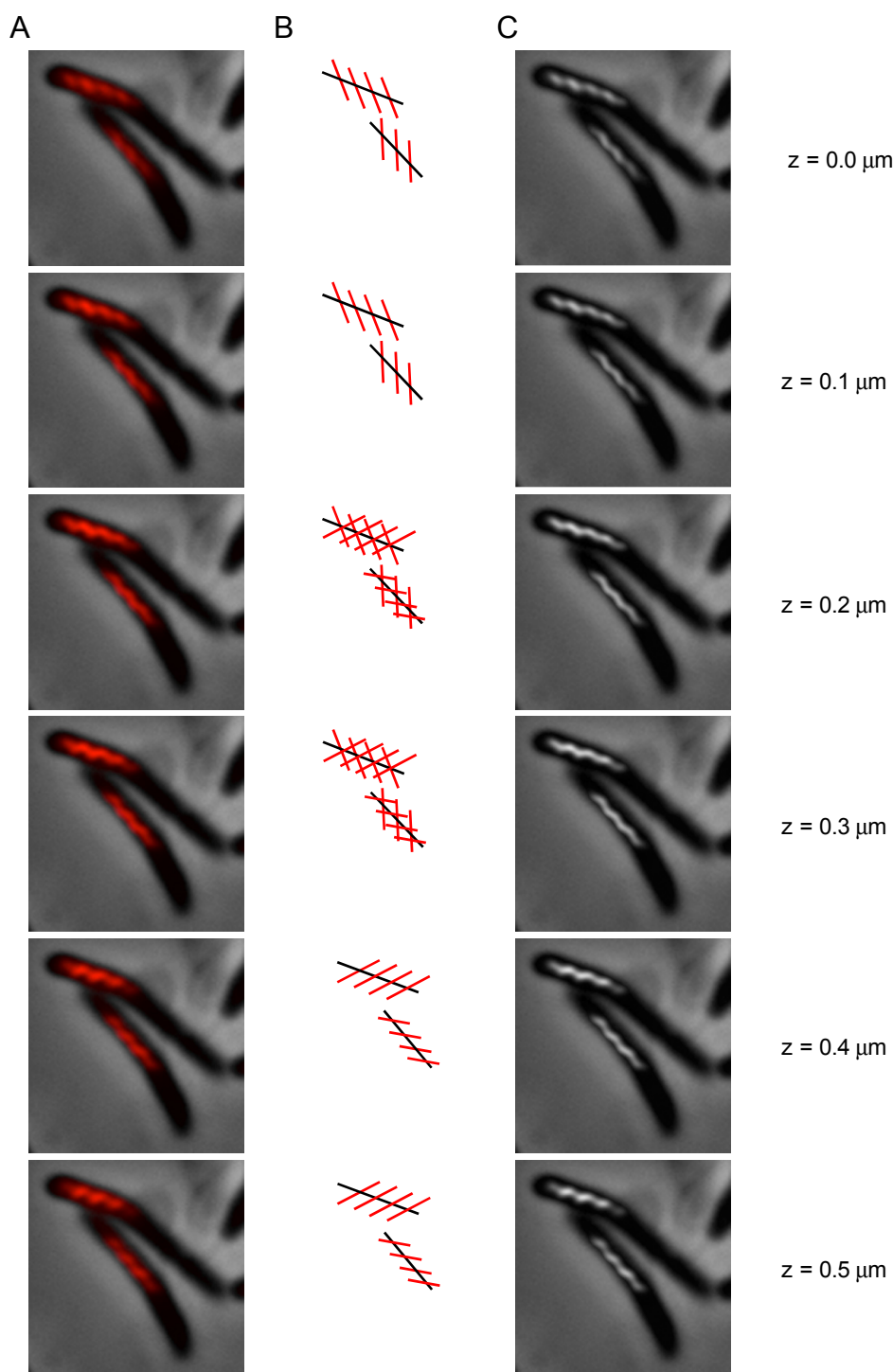


Fig. S10. Series of fluorescence images of EH364 cells producing BacM-mCherry screws. The images were recorded with $0.1 \mu\text{m}$ spacing starting at $0.0 \mu\text{m}$ and moving towards the bottom of the cell. The epifluorescence of the BacM-mCherry fusion protein was recorded after cells had been fixed with 4% formaldehyde for 10 hours. (A) Overlay of epifluorescence onto the phase contrast image of the cells. (B) Red lines across a black line indicate the directions of the visualized parts of the screws with respect to the screw axis. (C) Overlay of the epifluorescence signal after deconvolution onto the phase contrast image.

Conclusion: The way the orientations of the observed parts of the screws change when moving towards the bottom of the cell is consistent with a right handed helix. The helical pitch is $570 \pm 30 \text{ nm}$ ($N = 60$ helices).

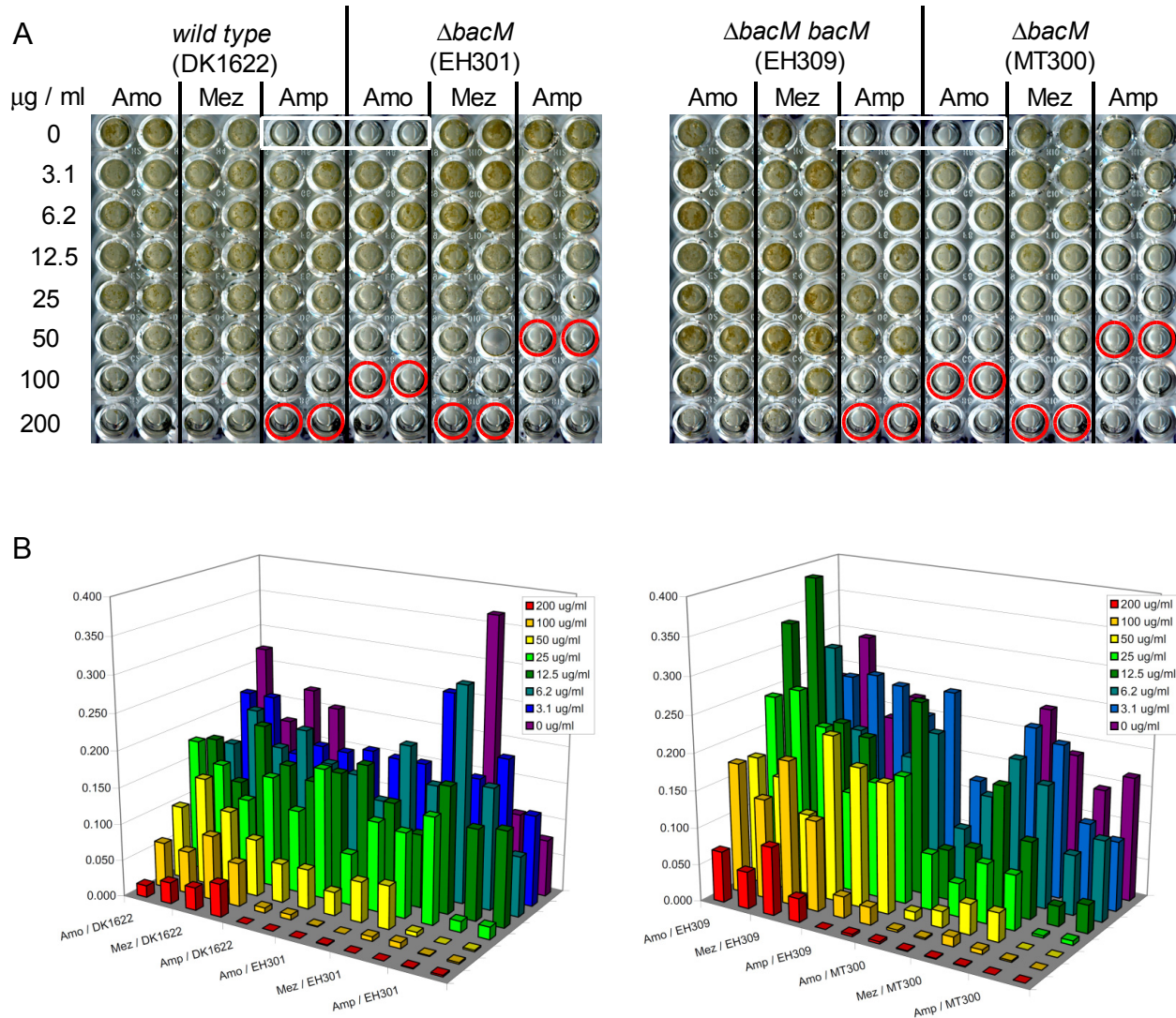


Fig. S11. Microtiter plate assay with different *M. xanthus* strains to determine their minimal inhibitory concentrations (MIC) for three antibiotics that target cell wall biosynthesis. (A) Scan of 96-well plates after 72 hours of incubation of cells containing or lacking BacM at 32°C, in the presence of different concentrations of antibiotics (relevant genotypes and strain names are indicated). Amo, amoxicillin; Mez, mezlocillin; Amp, ampicillin. Red circles mark the wells with no detectable cell growth after >3 days. The corresponding concentrations are the MICs for the respective combinations of strain and antibiotic. White boxes mark wells without cells. (B) Graphical depictions of the OD₆₀₀ values for the plates shown in A. Prior to the measurements, the contents of each well were resuspended by mixing with a pipet. Note that especially for the wells with higher cell densities, the OD₆₀₀ values are not accurately reflecting the amount of cells per well, due to a strong tendency of the cells to aggregate.

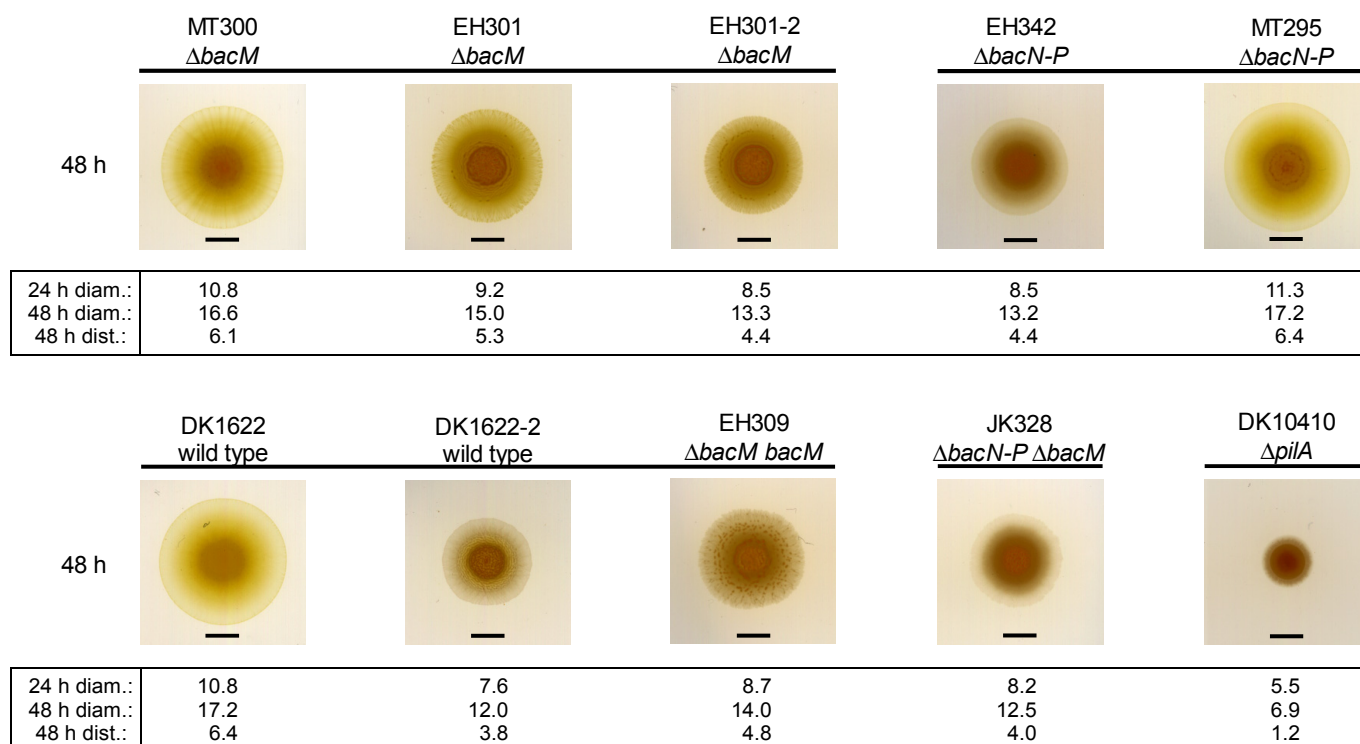


Fig. S12. S-motility assay. Swarming of *M. xanthus* strains on 0.4 % agar containing 50% CTT medium. All strains (genotypes indicated) were grown to an OD of 1.0 in CTT medium, pelleted and resuspended in CTT medium prior to spotting of 4 μ l cell suspension containing 2×10^7 cells. Plates were scanned after 48 hours. Bar represents 4.5 mm, the initial diameter of the cell spots. The $\Delta pilA$ strain exemplifies a lack of S-motility. Note that the variation between different clones of the same genotype (MT300, EH301, and EH301-2; EH342 and MT295; DK1622, DK1622-2, and EH309) can be of the same magnitude as the variation between strains with different genotypes (DK1622 and EH301; DK1622 and EH342; DK1622 and JK328). However, all strains except the S-motility-deficient strain DK10410 are clearly swarming on 0.4% agar plates. Diameters (diam.) of swarm areas after 24 and 48 hours, and distances (dist.) covered from the initial spot borders to the spot borders at 48 hours are listed below each scan (in mm).

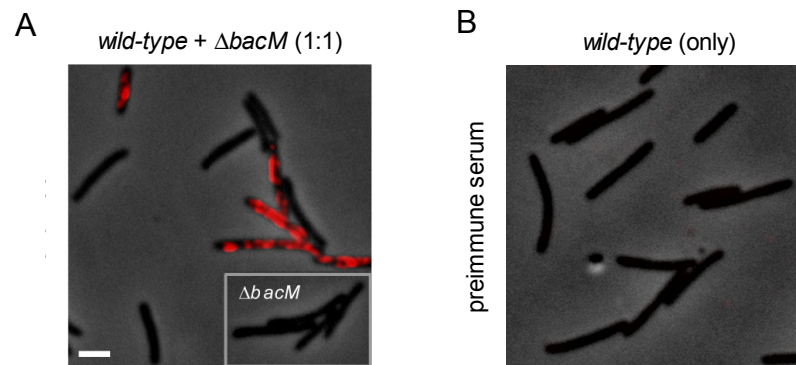


Fig. S13. (A) The specificity of purified anti-BacM antibody in immunofluorescence experiments is demonstrated with a 1:1 mixture of wild-type (strain DK1622) and $\Delta bacM$ cells (strain EH301), in which only half of the cells produced fluorescence when using Alexa594-coupled anti-rabbit IgG secondary antibody. No fluorescence was seen when only $\Delta bacM$ cells were used (inset). All of the cells showed fluorescence when using wild-type cells only (Fig. S7A). (B) Wild-type cells incubated with preimmune serum instead of anti-BacM antibody.

Table S2. Plasmids and primers used in this study.

Plasmid	Relevant description	Source or reference
pBJ114	Kan ^R , <i>galK</i> . Used for constructing gene replacements.	Julien <i>et al.</i> (2000), Ueki <i>et al.</i> (1996)
pSWU30	Tet ^R , <i>attP</i> . Used for inserting genes into the chromosomal phage Mx8 integration site <i>attB</i> .	Wu and Kaiser (1995)
pCR2.1-TOPO	Amp ^R , Kan ^R , TOPO cloning vector.	Invitrogen
pMKK203	pBJ114 with $\Delta bacM$ deletion cassette. For construction of strains EH301, EH302.	This study
pMKK205	pBJ114 with <i>bacM</i> complementation cassette. For construction of strains EH309, EH310, and EH368.	This study
pMKK212	pCR2.1-TOPO with <i>MXAN7474</i> disruption cassette. For construction of strain EH332.	This study
pMKK221	pBJ114 with $\Delta bacN$ - <i>P</i> deletion cassette. For construction of strains EH341 and EH342.	This study
pMKK222	pBJ114 with P _{<i>bacM</i>} - <i>bacM</i> - <i>mCherry</i> . For construction of strains EH351 and EH358.	This study
pMKK223	pSWU30 with P _{<i>pilA</i>} - <i>bacM</i> . For construction of strain and EH345.	This study
pMKK224	pSWU30 with P _{<i>oar</i>} - <i>bacM</i> . For construction of strain EH344.	This study
pMKK227	pSWU30 with P _{<i>oar</i>} - <i>bacM</i> - <i>mCherry</i> . For construction of strains EH362 and EH364.	This study
pET151/D-TOPO	Protein expression vector. Amp ^R	Invitrogen
pET151-7475FL	pET151 with <i>bacM</i> (<i>codon 1-151</i>)	This study
pET151-7475TR	pET151 with <i>bacM</i> (<i>codon 28-151</i>)	This study
pET151-Tag-7475TR	pET151 with <i>his₆-V5-TEV::bacM</i> (<i>codon 28-151</i>)	This study

Primers	Sequence ^a
US7475-2.seq	acct gaattc CCCTGCGCTGCTTGCG (EcoRI)
US7475-1.rev	GGAACGCACGTCTACTCTCTCTCT
DS7475-1.seq	GGAGTAGGACGTGCGTTCCTGGAAGC
DS7475-1.rev	tgc agaattc AGAAGCCAGGGCTCCG (EcoRI)
US4637-1.seq	tcat gaattc CCCGCTCCATCAGGCCATCG (EcoRI)
US4637-1.rev	GTCTTCTTCTTCCCGTTGCCATGCGGTGACC
DS4635-1.seq	TGGCAACGGGGAAGAAGAAGACCCGCTAGCG
DS4635-1.rev	cgata aagctt CTCGCTGCTCCGAACCTTCG (HindIII)
CORE7474-1.seq	tgaCCAGCTTCACTGCTGGCGCTC
CORE7474-1.rev	tcaGGGAGCTGCTCGCCGTCC
US7475-4.seq	accggctcttg AAGCTT ctcagg (HindIII)
7475-MCS-1.rev	cgctcgacctccccgggagctcgcttcttctcgccacccggagg
MCS-mCherry-1.seq	gctcgccccgggaggtcgacgggagcgggatccagATGGTGAGCAAGGGCGAGGAGG
COREmCherry-1.rev	agt caagttatctaga CTACTTGTACAGCTCGTCCATGC (HindIII, XbaI)
PpilA-2.seq	catgt ctaga TGAAGACCCGTGCTGCGGAG (XbaI)
PpilA-1.rev	ctgag gtacc TCCTCAGAGAAGGTTGCAACG (KpnI)
Poar-1.seq	tgact ctaga GTAGCCCCGACGCCGAATCG (XbaI)
Poar-1.rev	tcgag gtacc CCCCCAAGGTGGGCTGC (KpnI)
PpilA-7475-2.seq	CAACCTTCTCTGAGG gtacc GTGGCGCTCCTTGGCGGG (KpnI)
CORE7475-3.rev	gctag aatc GTCTACTTCTTCTCGCCACCC (EcoRI)
CORE7475-3.seq	CAACCT CGAG ACGCCGTCG (XhoI)
COREmCherry-2.rev	agt gaattc at ctaga CTACTTGTACAGCTCGTCCATGC (EcoRI, XbaI)
CM308.rev	CTACTTCTTCTCGCCACCCGG
CM309.seq	atatacatatgCGCTCCTTGGCGGG (NdeI)
CM310.rev	gatctgagctcgcccttCTACTTCTTCTCGCCACCCG (SacI)
CM311.seq	caccTCTGGTGAGGTCCACACG
CM312.seq	atatacatatgTCTGGTGAGGTCCACACG (NdeI)
CM327.seq	TGGGCGTCACTGCGTCA
CM328.rev	TTGAAGCCGGACAGGTGG
CM336.seq	CCTCTCACCATGTTTCTGACT
CM337.rev	ATGGATTTCGGAGAGCTCCTT
CM338.seq	AGAACCTGGCCAAGCAAGT
CM339.rev	GAGCACGTCTTTGGTGATGA
CM340.seq	TCATCACCAAAGACGTGCTC
CM341.rev	CGCCTGGAAGCTCTCATC

a. Bold highlighting marks restriction sites used for cloning, the respective enzymes are given in parentheses. Sequences in uppercase and lowercase represent sequences present within/adjacent to the respective genes in the genome, and additional sequences needed for cloning purposes, respectively. All sequences are given in 5' to 3' direction, with primers ending in 'seq' matching the direction of the respective gene, and those ending in 'rev' running into the opposite direction.

Construction of plasmids and strains

Table S2 lists the plasmids employed and the primers used for their construction. All *M. xanthus* mutants were obtained *via* electroporation of cells with 2–4 µg of plasmid DNA. In-frame deletions were generated via homologous recombination based on a previously described method (Ueki *et al.*, 1996). In brief, two DNA fragments corresponding to 300–400 bp, each, of the upstream and downstream regions of the target gene(s) were fused through overlap extension PCR and cloned into plasmid pBJ114 using appropriate restriction sites. Unless otherwise stated, genomic DNA from strain DK1622 was used as template for all PCR reactions. Plasmid insertion mutants were obtained by selecting for kanamycin resistance. Deletions were generated in these transformants by counterselection on CTT-agar plates containing 2.5% galactose. Galactose-resistant kanamycin-sensitive colonies were analyzed by PCR to confirm the respective deletion. The *bacM* deletions were further confirmed by immunoblot analysis, using purified anti-BacM antiserum, and *bacM* and *bacN-P* deletions were additionally confirmed via Southern blot analysis (data not shown). Complementation to restore the *bacM* wild-type locus were generated with the same strategy. All plasmids derived from pSWU30 contain the *attP* sequence from phage Mx8 and were integrated into the chromosomal *attB* site via a single crossover recombination event (Wu and Kaiser, 1995). The relevant genotypes of the generated strains were confirmed by PCR.

To construct $\Delta bacM$ strains, an in-frame deletion cassette was produced by fusing the PCR product of primers US7475-2.seq and US7475-1.rev to the product of primers DS7475-1.seq and DS7475-1.rev, followed by cloning of this fusion into the EcoRI site of pBJ114. The resulting plasmid **pMKK203** was used to transform strains DK1622 and DK8615 to eventually produce strains **EH301** and **EH302**, respectively.

To construct $\Delta bacN-P$ strains, an in-frame deletion cassette

was produced by fusing the PCR product of primers US4637-1.seq and US4637-1.rev to the product of primers DS4635-1.seq and DS4635-1.rev, followed by cloning of this fusion into EcoRI/HindIII-digested plasmid pBJ114. The resulting plasmid **pMKK221** was used to transform strains EH301 and DK1622 to eventually produce strains **EH341** and **EH342**, respectively.

To construct a *MXAN7474*-disruption strain, primers CORE7474-1.seq and CORE7474-1.rev were used to produce a PCR product, which was cloned into the commercial vector pCR2.1-TOPO according to the manufacturer's recommendations. The resulting plasmid **pMKK212** contained basepairs 25 to 264 of *MXAN7474*, framed by two in-frame TGA stop codons. It was used to transform strain DK1622 to produce strain **EH332**.

To complement *bacM* at the wild type locus, a PCR product comprising the sequence of the *bacM* gene plus 386 bp upstream of its start and 424 bp downstream of its stop codon was produced with primers US7475-2.seq and DS7475-1.rev. This fragment was cloned into the EcoRI site of pBJ114. The resulting plasmid **pMKK205** was used to transform strains EH301 and EH302 to eventually produce strains **EH309** and **EH310**. In these strains the *bacM* locus is restored to its wild-type state.

To introduce, at the wild-type locus of *bacM*, a gene encoding a fusion of *bacM* without its stop codon to a 39 bp linker sequence (GCGAGCTCGCCCGGGGAGGTGCGACGGGAGCGGGATCCAG) followed by the coding sequence of mCherry, the following strategy was employed: Plasmid pMKK205 was digested with EcoRI and HindIII. The two major fragments were purified and religated resulting in plasmid **pMKK222pre** which contains between its EcoRI and HindIII sites 362 bp of the upstream region of *bacM* up to the HindIII site 23 bp before the start of *bacM*. Subsequently, two PCR fragments were produced, one with primers US7475-4.seq and 7475-MCS-1.rev, one with MCS-mCherry-1.seq and CORE-mCherry-1.rev. These fragments were fused via overlap

extension PCR and cloned into HindIII-digested pMKK222pre producing plasmid **pMKK222**. Template for amplification of the *mCherry* gene was a plasmid carrying the gene. Plasmid pMKK222 contained 386 bp of upstream *bacM* sequence followed by the fusion of *bacM* to the linker sequence and the *mCherry* gene. The plasmid was used to transform strains DK1622, EH301, and EH302 to produce strains **EH351**, **EH358**, and **EH366**, respectively. The chromosomes of these strains now contain the fusion gene followed by the rest of the pMKK222 sequence, inserted at the wild-type *bacM* locus. In EH351, the plasmid DNA is followed by the complete wild-type genes *bacM* and *MXAN7474* under control of the *bacM* promoter, whereas in EH358, and in EH366 the wild-type *bacM* gene is absent.

To introduce *bacM* under control of the *pilA* promoter at the chromosomal *attB* site, the PCR product generated with primers PpilA-2.seq and PpilA-1.rev was fused via overlap extension to the PCR product generated with primers PpilA-7475-2.seq and CORE7475-3.rev. The resulting DNA fragment contained 300 bp of the sequence upstream of *pilA*, with the 6 bp immediately before *pilA* replaced with a KpnI site, followed by *bacM* and an EcoRI site. The fragment was cloned between the KpnI and EcoRI sites of pSWU30 to produce plasmid **pMKK223**, which was used to transform strain DK1622 to produce strain **EH345**.

To introduce *bacM* under control of the *oar* promoter at the chromosomal *attB* site, primers Poar-1.seq and Poar-1.rev were used to amplify 296 bp of the sequence upstream of *oar*, with the 6 bp immediately before *oar* replaced with a KpnI site. This DNA fragment was cloned between the XbaI and KpnI sites of pMKK223 to produce plasmid **pMKK224**, which was used to transform strain EH301 to produce strain **EH344**.

To introduce the above-described *bacM-mCherry* fusion gene under control of the *oar* promoter at the chromosomal *attB* site, the following strategy was applied: Primers CORE7475-3.seq and COREmCherry-2.rev were used

with plasmid pMKK222 as template to produce a PCR fragment which was cloned between the XhoI and EcoRI sites of pMKK224. The generated plasmid **pMKK227** was used to transform strains DK1622 and EH301 to produce strains **EH362** and **EH364**, respectively.

For the construction of *E. coli* strains which overproduce full-length (residues 1-150) or truncated (residues 28-150) versions of BacM, optionally with an N-terminal tag, the following strategy was used: For production of His6-V5-TEV-BacM⁽²⁸⁻¹⁵⁰⁾, DNA was amplified using reverse primer CM308.rev, and forward primer CM311.seq. The obtained PCR fragment was cloned in-frame into plasmid pET151/D-TOPO (Invitrogen) behind the region that encoded His6-tag, V5 epitope and TEV site, according to the recommendations of the supplier, to produce plasmid **pET151-Tag-7475TR**. For production of untagged proteins, DNA fragments were amplified using reverse primer CM310.rev, and either forward primer CM309.seq (BacM⁽¹⁻¹⁵⁰⁾) or CM312.seq (BacM⁽²⁸⁻¹⁵⁰⁾). PCR fragments were digested with NdeI and SacI and cloned between the NdeI and SacI sites of pET151/D-TOPO to produce plasmids **pET151-7475FL** and **pET151-7475TR**, respectively. Digestion of pET151/D-TOPO with these enzymes had removed the region encoding the His6 tag, V5 epitope, and TEV protease cleavage site, allowing for the production of untagged protein.

Each of the three constructs was used to transform *E. coli* TOP10 cells to allow for plasmid maintenance and confirmation via DNA sequencing. Subsequent transformations of *E. coli* BL21 Star (DE3) cells to generate strains **BL21-Tag-7475TR**, **BL21-7475FL** and **BL21-7475TR** allowed for expression of the encoded recombinant proteins.

MALDI-MS/MS analysis of in-gel trypsin-digested proteins

Coomassie Blue R250-stained gel bands were excised from an SDS PAGE gel, destained and digested with sequencing grade modified trypsin (Promega). Gel pieces were diced and washed for 10 min, each, in alternating 25 mM ammonium bicarbonate and 50% acetonitrile (ACN) until cleared of the stain. After drying the gel pieces in a vacuum centrifuge, in-gel protein digestion was performed in 20 - 30 μ l of a solution of 10 ng/ μ l trypsin in 25 mM ammonium bicarbonate for 14 hours at 37°C. After saving the supernatant, the gel pieces were extracted with 0.1% trifluoroacetic acid (TFA) followed by 50% ACN in 0.1% TFA. All supernatants were combined and dried in a vacuum centrifuge. Finally the peptides were redissolved in 8 μ l 33% ACN / 0.1% TFA. On a MALDI target, 0.5 μ l peptide solution was left to dry and 0.5 μ l of matrix solution (50 mg/ml dihydroxybenzoate in 50% ethanol / 0.1% TFA) was applied on top of the peptide spot. The dried mixtures were subjected to tandem mass spectrometry within a mass range of 0.7 to 4 kDa using a MALDI-LTQ mass spectrometer (Thermo Scientific) at the Johns Hopkins University mass spectrometry facility. Xcalibur software (Thermo Scientific) was used for data acquisition and visualization. Database searches were performed with a BioworksBrowser/Sequest software package (Thermo Scientific). Graphical assignment of the different peptides to their corresponding peaks in the peptide mass fingerprint spectra was performed manually.

References (not listed in the print version)

- Cordell, S. C., Anderson, R. E., and Löwe, J. (2001) Crystal structure of the bacterial cell division inhibitor MinC. *EMBO J* **20**: 2454-2461.
- Julien, B., Kaiser, A. D., and Garza, A. (2000) Spatial control of cell differentiation in *Myxococcus xanthus*. *Proc Natl Acad Sci USA* **97**: 9098-9103.
- Ueki, T., Inouye, S., and Inouye, M. (1996) Positive-negative KG cassettes for construction of multi-gene deletions using a single drug marker. *Gene* **183**: 153-157.